Macedonian Journal of Chemistry and Chemical Engineering, Vol. **37**, No. 2, pp. 173–184 (2018)

MJCCA9 – 758 ISSN 1857-5552
e-ISSN 1857-5625
Received: July 10, 2018 DOI: 10.20450/mjcce.2018.1503
Accepted: October 2, 2018 *Original scientific paper*

SYNTHESIS AND CHARACTERIZATION OF A NOVEL ISOCOUMARIN-DERIVED POLYMER AND THE INVESTIGATION OF ITS THERMAL DECOMPOSITION KINETICS

Adnan Kurt[1,*], Halil İbrahim Avcı[1], Murat Koca[2]

[1]*Department of Chemistry, Faculty of Science and Arts, Adiyaman University, Adiyaman, Turkey*
[2]*Department of Pharm. Chemistry, Pharmacy Faculty, Adiyaman University, Adiyaman, Turkey*
akurt@adiyaman.edu.tr

A novel isocoumarin-derived polymer, poly(2-(isocoumarin-3-yl)-2-oxoethyl methacrylate) (poly(ICEMA)), was synthesized by free radical polymerization. A spectral characterization was performed with FTIR, ^{1}H and ^{13}C-NMR spectroscopies. The glass transition temperature of poly(ICEMA) was measured to be 161.69 °C by DSC. The initial decomposition temperatures obtained from TGA showed a change in the positive direction from 256.59 to 286.10 °C as the heating rate increased to 20 °C/min. The thermal decomposition activation energies of poly(ICEMA) in the conversion range of 7–19% were found to be 136.12 and 134.83 kJ/mol by the Flynn–Wall–Ozawa and Kissinger models, respectively. In addition, various integral models, such as the Coats-Redfern, Tang, Madhusudanan and Van Krevelen models, were used to determine the thermal decomposition mechanism of poly(ICEMA), which showed that it proceeded at the optimum heating rate of 5 ºC/min over the D_1 one-dimensional diffusion-type deceleration mechanism.

Keywords: isocoumarin polymer; synthesis and characterization; thermal decomposition kinetics; activation energy

СИНТЕЗА И КАРАКТЕРИЗАЦИЈА НА НОВ ПОЛИМЕР ИЗВЕДЕН ОД ИЗОКУМАРИН И ИСПИТУВАЊЕ НА КИНЕТИКАТА НА НЕГОВОТО ТЕРМИЧКО РАЗЛОЖУВАЊЕ

По пат на слободнорадикалска полимеризација е синтетизиран нов полимер изведен од изокумарин, поли(2-изокумарин-3-ил)-2-оксоетил метакрилат) (poly(ICEMA)). Спектралната карактеризација е извршена со FTIR, ^{1}H и ^{13}C-NMR. Со DSC е измерно дека температурата на транзиција во стакло на poly(ICEMA) е 161,69 °C. Иницијалната температура на разложување со TGA покажува промена во позитивна насока од 256,59 до 286,10 °C со покачување на степенот на загревање до 20 °C/min. Измерено е дека активационата енергија на термичкото разложвуање на poly(ICEMA) во опсегот на претворба од 7–19 % според моделите на Flynn–Wall–Ozawa и Kissinger изнесува соодветно 136,12 и 134,83 kJ/mol. Исто така, за да се определи механизмот на термичкото разложување на poly(ICEMA), беа користени разни интегрални модели како што се Coats-Redfern, Tang, Madhusudanan и Van Krevelen што покажа дека оптимална брзина на загревање е 5 ºC/min поради D_1 еднодимензионален забавувачки механизам од дифузен тип.

Клучни зборови: изокумаринcки полимер; синтеза и карактеризација; кинетика на термичко разложување; активационата енергија

1. INTRODUCTION

α-Pyranone (2H-pyran-2-one) is a six-membered oxygen heterocyclic compound and is an important member of natural compounds containing an unsaturated lactone ring [1–3]. Isocoumarins, as a new class of heterocyclic compounds, are obtained by bonding the benzo-group to the α-pyranone ring [2]. These compounds are structurally similar to coumarins, which are also lactone-derived compounds commonly found in nature, and show structural isomerism with these compounds [1]. In addition, similar to coumarin compounds, the isocoumarins and their derivatives with the same aromatic lactone ring attract a great deal of attention due to their abundance in nature and also their physical, chemical and biological properties [3–5]. In particular, they have potential use in many fields thanks to their unique and special chemical structures containing the heterocyclic π-conjugated system [4]. Isocoumarins have a wide range of pharmacological activities, including antifungal [6], anti-inflammatory [7], antimicrobial [8], phytotoxic [9] and cytotoxic [10] properties. Furthermore, isocoumarins are used as reagents in the synthesis of many important hetero and carboxylic compounds, including isocarbostyrils, isoquinolines, isochromenes and different aromatics [2, 5].

In addition to their natural presence and extraction from various plants, the synthesis of these compounds and new derivatives not found in nature has also been well performed in laboratory conditions in recent years. With the exception of the conventional methods used for the synthesis of these compounds, transition metal catalyzed reactions have recently been attempted [5]. Transition metal catalyzed reactions for the synthesis of isocoumarin derivatives, in particular salts of transition metals, such as Cu, Pd, Ag, Ru, Rh and Ir, or their complexes are noteworthy [1]. Furthermore, other synthetic methods, such as insertion, cyclization and bond cleavage reactions, are possible [5].

Alternatively, a large number of polymers with different reactive functional groups have successfully been synthesized and tested to date [11–16]. These polymers are used not only for their macromolecular properties, but also for their specific applications due to their functional properties [12, 17]. However, nearly all of the studies performed on isocoumarins are directed to the obtaining of small molecules with organic synthesis [1–3, 5]. Based on our literature knowledge, we have not found any studies that develop isocoumarin-derived methacrylate polymers and investigate the thermal decomposition kinetics of these polymeric materials. Therefore, in present study, we aim to synthesize and characterize a novel isocoumarin-derived polymer, poly(2-(isocoumarin-3-yl)-2-oxoethyl methacrylate) (poly(ICEMA)), and investigate its thermal decomposition kinetics by various kinetic models in the studied conversion range.

2. EXPERIMENTAL

2.1. *Materials*

2-Carboxybenzaldehyde, chloroacetone, bromine (reagent grade), glacial acetic acid, sodium methacrylate, triethylamine, sodium methacrylate, tetrahydrofuran (THF), N,N-dimethylformamide (DMF), chloroform, ethanol, sodium hydroxide and anhydrous magnesium sulfate were purchased from Sigma-Aldrich. Azobisisobutyronitrile (AIBN) used as an initiator for polymerization was purchased from MERC and it was dissolved in chloroform and then recrystallized from ethanol.

2.2. *Instrumental techniques*

NMR spectra of the compounds were recorded on a Bruker 300 MHz Ultrashield TM instrument at room temperature using a deuterated DMSO solvent and TMS as an internal standard. The infrared characterization of compounds was carried out using a Perkin Elmer Spectrum 100 FTIR spectrometer with an ATR accessory. A Perkin Elmer DSC 8000 was used to determine the glass transition temperature of poly(ICEMA) in the temperature range of 30–250 ºC at a heating rate of 20 ºC/min under a nitrogen atmosphere. TGA experiments were performed with a Seiko SII 7300 TG/DTA under a dynamic nitrogen gas atmosphere of 25 ml/min flow rate with heating rates of 5, 10, 15 and 20 °C/min over a range of temperatures from 30 to 500 ºC.

2.3. *Synthesis of 3-acetyl isocoumarin*

2-Carboxybenzaldehyde (2.33 g, 1.53 mmol), chloracetone (0.14 g, 1.53 mmol) and triethylamine (0.15 g, 1.53 mmol) were added into a three-necked reaction flask. After setting the ambient temperature to 130 °C, the reaction was carried out in solvent-free media for 3 h, as reported by Koca et al. [18]. The obtained crude product was precipitated in pure water and then dried at room temperature. Finally, 3-acetyl isocoumarin compound (1) was purified by crystallization from ethyl alcohol.

FTIR (cm^{-1}): 3088–3048 (aromatic C-H stretching), 3003–2881 (aliphatic C-H stretching),

1721 (acetyl ketone C=O stretching), 1678 (isocoumarin C=O stretching), 1643 (isocoumarin aliphatic C=C stretching), 1600 (aromatic C=C stretching) and 1086 (C-O-C stretching).

^{1}H-NMR ($CDCl_3$, δppm): 8.39 (isocoumarin =CH- proton), 7.86–7.42 (aromatic =CH- protons) and 2.61 (acetyl -CH_3 protons).

^{13}C-NMR ($CDCl_3$, δppm): 192.21 (acetyl ketone carbonyl carbon), 160.93 (isocarbonyl carbonyl carbon), 149.39 (ipso carbon next to acetyl group), 135.31–109.02 (aromatic and aliphatic C=C carbons) and 26.18 (acetyl -CH_3 carbon).

2.4. *Synthesis of 3-(2-bromoacetyl) isocoumarin*

For the bromination process, 3-acetyl isocoumarin (0.5 g, 1.87 mmol) and glacial acetic acid (50 ml) were added to a three-necked reaction flask to dissolve the isocoumarin compound and the reaction medium temperature was then set to 5 °C. Alternatively, the liquid bromine (Br_2, 0.3 g, 1.87 mmol) dissolved in 20 ml of glacial acetic acid was added dropwise to the 3-acetyl isocoumarin solution. After the addition of bromine solution was finished, the mixture was stirred with a magnetic stirrer for 24 h at room temperature. The reaction mixture was then precipitated in pure water. The obtained product was crystallized from acetic acid to synthesize pure 3-(2-bromoacetyl) isocoumarin compound (2).

FTIR (cm^{-1}): 3118–3031 (aromatic C-H stretching), 2986–2888 (aliphatic C-H stretching), 1724 (acetyl ketone C=O stretching), 1705 (isocoumarin C=O stretching), 1680 (isocoumarin aliphatic C=C stretching) and 1598 (aromatic C=C stretching).

^{1}H-NMR ($CDCl_3$, δppm): 8.40 (isocoumarin =CH- proton), 7.87–6.88 (aromatic =CH- protons) and 4.50 (acetyl –CH_2Br protons).

2.5. *Synthesis of 2-(isocoumarin-3-yl)-2-oxoethyl methacrylate monomer*

3-(2-bromoacetyl) isocoumarin (0.5 g, 1.87 mmol), sodium methacrylate (0.205 g, 1.90 mmol), THF (50 ml) and hydroquinone as an inhibitor (trace amount) were added into a three-necked reaction flask, which was then heated under reflux for 24 h on a heated magnetic stirrer. After the reaction was completed, the reaction mixture was filtered and the THF solvent was removed in vacuum. The crude product was then purified by precipitation in pure water. The resulting ICEMA monomer (3) was dried at room temperature.

FTIR (cm^{-1}): 3111–3041 (aromatic C-H stretching), 2993–2853 (aliphatic C-H stretching), 1741 (methacrylate C=O stretching), 1722 (acetyl ketone C=O stretching), 1708 (isocoumarin C=O stretching), 1672 (isocoumarin aliphatic C=C stretching), 1634 (vinyl C=C stretching) and 1601 (aromatic C=C stretching).

^{1}H-NMR (DMSO, δppm): 8.27 (isocoumarin =CH- proton), 8.01–7.78 (aromatic =CH- protons), 6.17 and 5.82 (vinyl =CH_2 protons), 5.45 (–OCH_2 protons next to methacrylate ester carbonyl), 1.95 (-CH_3 protons next to vinyl group) and 3.35 and 2.50 (DMSO solvent protons).

^{13}C-NMR (DMSO, δppm): 186.42 (ketone carbonyl carbon next to isocoumarin group), 165.86 (methacrylate ester carbonyl carbon), 159.89 (isocoumarin carbonyl carbon), 146.91 (ipso carbon at 3th position of coumarin), 135.66–111.10 (aromatic and aliphatic C=C carbons), 66.00 (–OCH_2 carbon next to methacrylate ester), 17.96 (vinyl -CH_3 carbon) and 39.46 (DMSO solvent).

2.6. *Synthesis of poly(2-(isocoumarin-3-yl)-2-oxoethyl methacrylate) homopolymer*

Homopolymerization of the ICEMA monomer was achieved using the free radical polymerization method. To this end, ICEMA monomer (0.4 g), AIBN initiator (0.040 g, 10 % wt. monomer) and DMF solvent (2 ml) were added to a polymerization tube, respectively. After dissolving the reagents, the solution was purged with nitrogen gas for 10 min. The tube was then closed and immersed in an oil bath previously set to 60 °C. The polymerization time was continued for 48 h. The polymer solution was precipitated in ethanol and then filtered and dried at 40 °C to obtain poly(2-(isocoumarin-3-yl)-2-oxoethyl methacrylate) homopolymer (4), poly(ICEMA). A schematic representation of the polymer synthesis is shown in Scheme 1.

FTIR (cm^{-1}): 3132–3020 (aromatic C-H stretching), 2996–2898 (aliphatic C-H stretching), 1739 (methacrylate C=O stretching), 1722 (acetyl ketone C=O stretching), 1715 (isocoumarin C=O stretching), 1671 (isocoumarin aliphatic C=C stretching) and 1601 (aromatic C=C stretching).

^{1}H-NMR (DMSO, δppm): 8.26 (isocoumarin =CH- proton), 7.95–6.64 (aromatic =CH- protons), 5.39 (–OCH_2 protons next to methacrylate ester carbonyl), 2.27 and 1.28 (methylene and methyl protons in polymer main chain) and 3.35 and 2.50 (DMSO solvent protons).

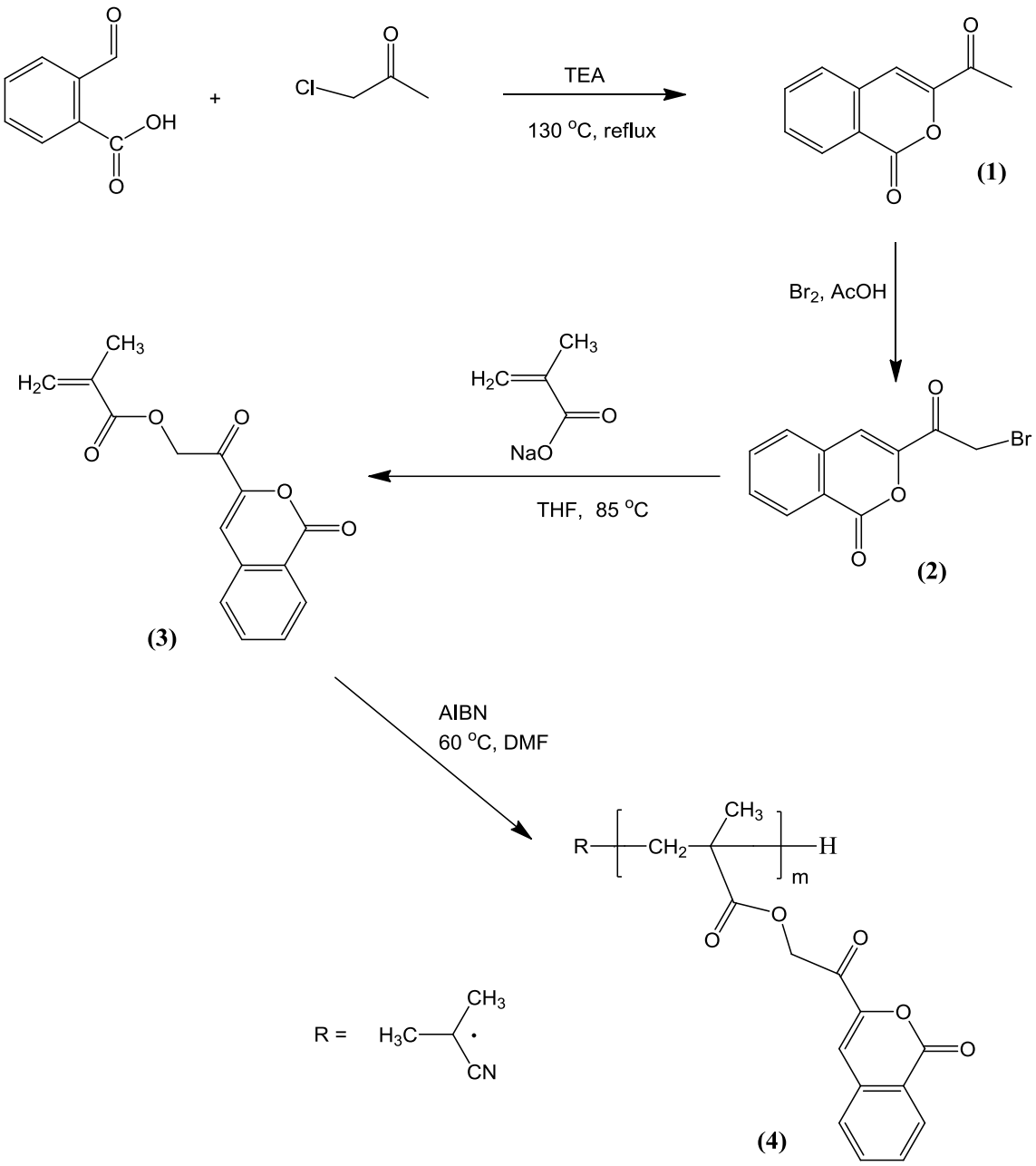

Scheme 1. Synthesis of poly(2-(isocoumarin-3-yl)-2-oxoethyl methacrylate)

3. RESULTS AND DISCUSSION

Figure 1(a) shows the FTIR spectrum of the ICEMA monomer, where the most characteristic absorption bands are observed at 3111–3041 cm^{-1} for aromatic C-H stretching, 2993–2853 cm^{-1} for aliphatic C-H stretching, 1741 cm^{-1} for methacrylate C=O stretching, 1722 cm^{-1} for acetyl ketone C=O stretching, 1708 cm^{-1} for isocoumarin C=O stretching, 1672 cm^{-1} for isocoumarin aliphatic C=C stretching, 1634 cm^{-1} for vinyl C=C stretching and 1601 cm^{-1} for aromatic C=C stretching. In the ^{1}H-NMR spectrum of the ICEMA monomer, as shown in Figure 2(a), the observed chemical shifts are attributed to the =CH- proton in the isocoumarin ring at 8.27 ppm, to aromatic =CH- protons at the chemical shift range of 8.01 to 7.78 ppm, to the vinyl $=CH_2$ protons at 6.17 and 5.82 ppm, to -$COOCH_2$- protons next the methacrylate ester at 5.45 ppm, to the -CH_3 protons adjacent to the vinyl group at 1.95 ppm, and the 3.35 and 2.50 ppm signals are also attributed to the DMSO solvent protons.

The synthesized isocoumarin-derived polymer, poly(ICEMA), was also characterized by FTIR and ^{1}H-NMR techniques. The FTIR spectrum of poly(ICEMA) is shown in Figure 1(b).

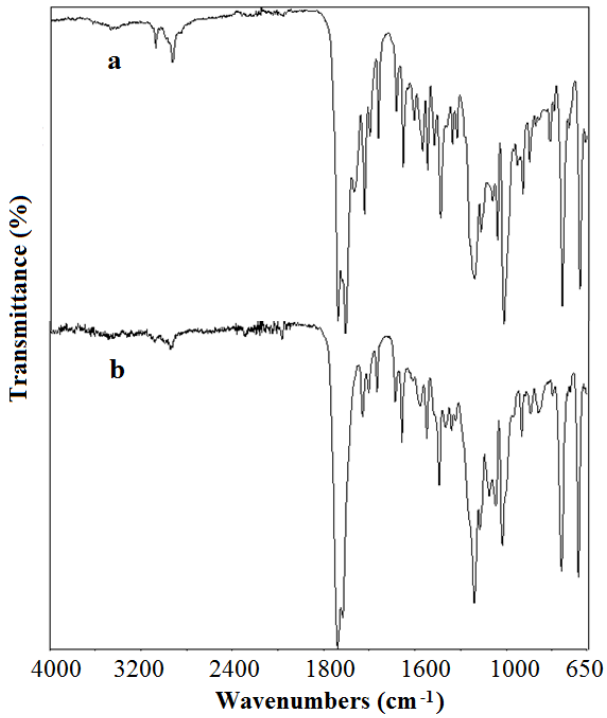

Fig. 1. FTIR spectra (a) ICEMA monomer and (b) poly(ICEMA) homopolymer

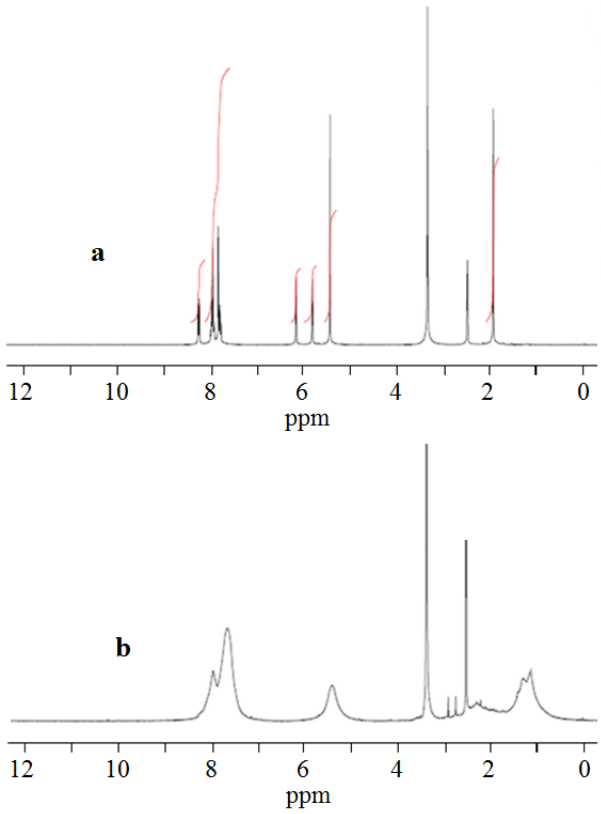

Fig. 2. ^{1}H-NMR spectra of (a) ICEMA monomer and (b) poly(ICEMA) homopolymer

The vibration bands at 3132–3020 and 2996–2898 cm^{-1} are characteristic for aromatic and aliphatic C-H stretching, respectively. The methacrylate ester carbonyl stretching is observed at 1739 cm^{-1}, whereas the acetyl ketone carbonyl and isocoumarin carbonyl stretching is at 1722 and 1715 cm^{-1}, respectively. At the frequency region of C=C stretching in this spectrum, only the absorption bands at 1671 and 1601 cm^{-1} reasoned from isocoumarin aliphatic C=C and aromatic C=C stretching are seen. As expected, the vinyl C=C stretching at 1634 cm^{-1} (for the monomer) disappeared by polymerization and this is one of main evidences that the homopolymerization of ICEMA is accomplished by the free radical polymerization method [14].

In the ^{1}H-NMR spectrum of the poly (ICEMA) polymer (Fig. 2(b)), the chemical shift at 8.26 ppm is attributed to the isocoumarin =CH- proton. The signal groups between 7.95 and 6.64 ppm are due to aromatic =CH- protons. The singlet signal at 5.39 ppm is assigned to the –OCH_2 protons next to methacrylate ester carbonyl. By the polymerization, two vinylic =CH_2 protons present in the monomer at 6.17 and 5.82 ppm disappear and these signals are moved to 2.27–1.28 ppm of homopolymer backbone methylene and methyl proton scale. This is also another main evidence that the homopolymerization of ICEMA is accomplished by the free radical polymerization method.

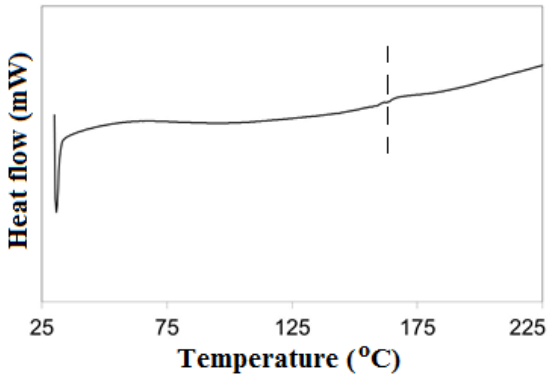

Fig. 3. DSC curve of poly(ICEMA) homopolymer

The glass transition temperature (*Tg*) of poly(ICEMA) was determined by using differential scanning calorimetry technique (DSC) and its thermogram is illustrated in Figure 3. As can be seen from that thermogram, the tg of poly(ICEMA) was measured to be 161.69 °C. We can compare this value only to that of coumarin-derived polymers (as the isomer of isocoumarin), since the isocoumarin containing polymers cannot be found in the literature according to our literature knowledge. The *Tg* value of poly(ICEMA) is agreement with the *Tg* values recorded for the couma-

rin-derived polymers in the literature. For example, in one study, Fomine and coworkers reported that the *Tg* values of some coumarin polymers are shifted in the range of 100–230 °C [19]. In addition, in our previous studies, we have found that the *Tg* of a coumarin-derived polymer, poly(poly(3-benzoyl coumarin-7-yl-methacrylate), to be 179 °C [13], and in another study, it is determined to be 176 °C for another coumarin, polymer poly(3-acetylcoumarin-7-ylmethacrylate) [14].

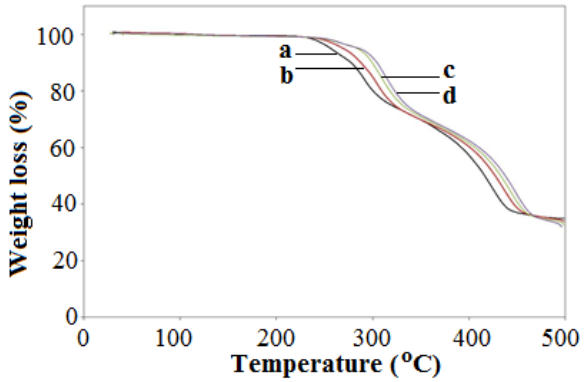

Fig. 4. TGA curves of poly(ICEMA) at different heating rates of a) 5 °C/min, b) 10 °C/min, c) 15 °C/min and d) 20 °C/min

The thermal behavior of the poly(ICEMA) homopolymer was investigated in detail using thermogravimetric analysis (TGA). For this purpose, poly(ICEMA) samples were heated from ambient temperature at 500 °C at different heating rates of 5, 10, 15 and 20 °C/min in a nitrogen gas atmosphere. TGA thermograms of poly(ICEMA) recorded at different heating rates are shown comparatively in Figure 4. Decomposition is observed at two stages, with up to 30% weight loss attributed to the formation of volatile hydrocarbons at ~350 °C and the second decomposition stage is approximately between 350 and 450 °C, with up to 65 % weight loss. This decomposition range is consistent with the thermal decomposition values of coumarin polymers. Patel and co-workers determined that the thermal decomposition of a series of coumarin containing polyacrylates occurred at the temperature range of 263–458 °C [17]. In addition, some thermal characteristics, such as the initial and final decomposition temperatures, the weight losses at different temperatures and the temperature of semi-weight loss, are given in Table 1. It can be seen that the initial decomposition temperatures (accepted as 5 % weight loss) of poly(ICEMA) at heating rates of 5, 10, 15 and 20 °C/min are measured as 256.59, 269.61, 285.36 and 286.10 °C, respectively. As the heating rate increases, the decomposition temperatures show a change in the positive direction [13, 16, 20].

T a b l e 1

Thermal behaviors of poly(ICEMA) at different heating rates

Reaction rate (°C/min)	T_a (°C)	T_b (°C)	%Weight loss at 300 °C	%Weight loss at 400 °C	Residue at 500 °C (%)
5	256.59	416.90	19.82	42.70	65.06
10	269.61	427.26	15.09	39.64	66.06
15	285.36	433.18	10.25	38.46	67.39
20	286.10	437.71	8.22	37.54	67.99

T_a and T_b: Decomposition temperatures at the weight losses of 5% and 50%, respectively

Thermal decomposition reactions of solid-state materials are defined by the following expression [21]:

$$\frac{d\alpha}{dt} = A\, exp\left(-\frac{E}{RT}\right) f(\alpha) \qquad (1)$$

where k(T) is a temperature-dependent rate constant, $f(\alpha)$ is the particular reaction model describing the dependence of the reaction rate on the extent of reaction, α represents the extent of reaction, which can be determined from TGA runs as a fractional mass loss, t is time, and A and E are the pre-exponential factor and activation energy, respectively.

Furthermore, $g(\alpha)$ is defined as the integral function of conversion as expressed by the following equation:

$$g(\alpha) = \int_0^{\alpha_p} \frac{d\alpha}{f(\alpha)} = \frac{A}{\beta} \int_0^{T_p} e^{-\frac{E}{RT}}\, dT \qquad (2)$$

where R is the ideal gas constant, β is the heating rate and T is the absolute temperature. Thermal decomposition of polymeric materials generally follows one of the decomposition processes of a sigmoidal and deceleration-type mechanism [22].

Various statements of $g(\alpha)$ integral functions are given in Table 2 and by using these functions, thermal decomposition mechanisms may easily be determined by TGA [23].

T a b l e 2

Algebraic expressions for g(α) for the most frequently used mechanisms of solid state processes

Symbol	g(α)	Solid state processes
Sigmoidal curves		
A_2	$[-\ln(1-\alpha)]^{1/2}$	Nucleation and growth (Avrami equation 1)
A_3	$[-\ln(1-\alpha)]^{1/3}$	Nucleation and growth (Avrami equation 2)
A_4	$[-\ln(1-\alpha)]^{1/4}$	Nucleation and growth (Avrami equation 3)
Deceleration curves		
R_1	α	Phase boundary controlled reaction (One-dimensional movement)
R_2	$[1-(1-\alpha)^{1/2}]$	Phase boundary controlled reaction (contraction area)
R_3	$[1-(1-\alpha)^{1/3}]$	Phase boundary controlled reaction (contraction volume)
D_1	α^2	One-dimensional diffusion
D_2	$(1-\alpha)\ln(1-\alpha)+\alpha$	Two-dimensional diffusion
D_3	$[1-(1-\alpha)^{1/3}]^2$	Three-dimensional diffusion (Jander equation)
D_4	$(1-2/3\alpha)\ (1-\alpha)^{2/3}$	Three-dimensional diffusion (Ginstling-Brounshtein equation)
F_1	$-\ln(1-\alpha)$	Random nucleation with one nucleus on the individual particle
F_2	$1/(1-\alpha)$	Random nucleation with two nuclei on the individual particle
F_3	$1/(1-\alpha)^2$	Random nucleation with three nuclei on the individual particle

The thermal decomposition activation energies of the ICEMA homopolymer have been determined according to the Flynn-Wall-Ozawa [24,25] and Kissinger [26] methods using the data obtained from TGA thermograms at different heating rates. Both of these methods are especially used to determine activation energies because they are integral methods and do not require any knowledge of the reaction order or the decomposition mechanism of the polymer [23]. The Flynn-Wall-Ozawa method uses the following equation:

$$\log \beta = \log\left[\frac{AE}{g(\alpha)\mathrm{R}}\right] - 2.315 - \frac{0.457\,E}{\mathrm{R}T} \tag{3}$$

where E is the activation energy calculated from the slope of log β versus (1000/T) plots. Another integral method is the Kissinger method, expressed as follows:

$$\ln\left(\frac{\beta}{T_{\max}^2}\right) = \left\{\ln\frac{\mathrm{AR}}{E} + \ln\left[n(1-\alpha_{\max})^{n-1}\right]\right\} - \frac{E}{\mathrm{R}T_{\max}} \tag{4}$$

where $T_{\max}$ is the temperature corresponding to the maximum reaction rate, $\alpha_{\max}$ is the maximum conversion at $T_{\max}$ and n is the reaction order. The activation energy, E, can be calculated from the slope of a plot of $\ln(\beta/T^2_{\max})$ versus $1000/T_{\max}$.

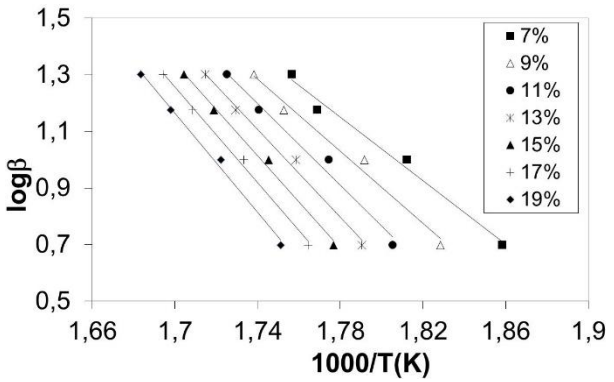

Fig. 5. Flynn-Wall-Ozawa lines at different conversion values

The measurements at conversion values of 7 %, 9 %, 11 %, 13 %, 15 %, 17 % and 19 % are obtained for the Flynn-Wall-Ozawa method. The logβ against 1000/T values determined at the above conversions are plotted in Figure 5. From the slope of a series line, the activation energy values corresponding to each conversion percentage have been separately calculated and given in Table 3. The average activation energy value for the poly(ICEMA) homopolymer among these values is calculated to be 136.12 kJ/mol. The closest value to the calculated average activation energy value is also obtained at the conversion of 11% with a value of 131.51 kJ/mol.

T a b l e 3

Activation energies of poly(ICEMA) calculated by Flynn-Wall-Ozawa method

α (%)	*E* (kJ/mol)	*R*
7	102.06	0.986
9	115.98	0.984
11	131.51	0.981
13	141.12	0.991
15	148.60	0.994
17	153.80	0.995
19	159.80	0.993
Mean	136,12	

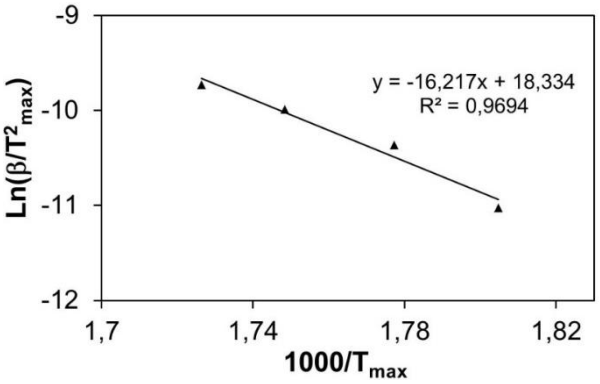

Fig. 6. $\ln(\beta/T^2_{max})$ versus $1000/T_{max}$ plots obtained from Kissinger method.

The $\ln(\beta/T^2_{max})$ versus $1000/T_{max}$ plots obtained at different heating rates for the Kissinger method, another method that is independent of reaction order, is shown in Figure 6. The temperatures (T_{max}) corresponding to the maximum decomposition rate required to calculate the activation energy value according to this method have been measured from the derivative thermogravimetry (DTG) as 280.91, 289.49, 298.81 and 306.10 °C at heating rates of 5, 10, 15 and 20 ° C/min, respectively.

From the slope of the curve shown in Figure 5, the activation energy is calculated as 134.83 kJ/mol. There is an energy difference of 1.29 kJ/mol between the thermal decomposition activation energy values calculated according to Flynn-Wall-Ozawa and Kissinger methods. This result shows that the activation energies obtained from both methods are in good agreement with each other.

In order to determine the thermal degradation mechanism of the ICEMA homopolymer, the activation energy values calculated from the kinetic methods of Coats-Redfern [27], Tang [28], Madhusudanan [29] and Van Krevelen [30] have been compared with the activation energies obtained from the Flynn-Wall-Ozawa and Kissinger integral methods. By using these kinetic methods, the accuracy of the measurements for calculating the thermal decomposition mechanisms of poly(ICEMA) will have been increased. These kinetic methods are briefly described below.

One of these kinetic methods is suggested by Coats-Redfern, as represented by the following equation:

$$\ln \frac{g(\alpha)}{T^2} = \ln \frac{AR}{\beta E} - \frac{E}{RT} \tag{5}$$

The apparent activation energies of each g(α) function can be determined from a plot of $\ln[g(\alpha)/T^2]$ versus 1000/T according to the various decomposition processes. In addition to the Coats-Redfern method, thermal decomposition mechanism of poly(ICEMA) is expressed by the Tang method as below:

$$\ln\left[\frac{g(\alpha)}{T^{1.89466100}}\right] = \left[\ln \frac{AE}{\beta R} + 3.63504095 - 1.89466100 \ln E\right] - 1.00145033 \frac{E}{RT} \tag{6}$$

where the activation energy is calculated from the slope of the plots of $\ln[g(\alpha)/T^{1.89466100}]$ versus 1000/T for every g(α) function. Another kinetic method to determine the decomposition mechanism of poly(ICEMA) is suggested by Madhusudanan in the following equation:

$$\ln\left[\frac{g(\alpha)}{T^{1.921503}}\right] = \left[\ln \frac{AE}{\beta R} + 3.772050 - 1.921503 \ln E\right] - 1.000955716 \frac{E}{RT} \tag{7}$$

The slope of $\ln[g(\alpha)/T^{1.921503}]$ versus 1000/T plots gives the activation energies of each $g(\alpha)$ function. Additionally, the Van Krevelen method may be used to verify the thermal decomposition mechanism of poly(ICEMA) by the following equation:

$$\log g(\alpha) = \log B + \left(\frac{E}{RT_r} + 1\right)\log T \quad (8)$$

where T_r is a reference temperature that represents the maximum temperature rate obtained by derivative thermogravimetric analysis. The slope of log $g(\alpha)$ versus log$T$ plots gives the activation energies for each $g(\alpha)$ function.

The thermal decomposition activation energies and linear regressions for various statements of $g(\alpha)$ integral functions determined in the range of 9–21 % are summarized in Tables 4 to 7 for the used kinetic models at heating rates of 5, 10, 15 and 20 ºC/min. When these tables are examined, the deceleration-type dimensional diffusion mechanisms (D_n) are evident in all methods because the activation energies calculated for these deceleration-type mechanisms are very close to the activation energies calculated from the Flynn-Wall-Ozawa (E = 136.12 kJ/mol) and Kissinger (E = 134.83 kJ/mol) methods.

T a b l e 4

Activation energies obtained for several solid-state processes at different heating rates using the Coats-Redfern method

Mechanism	Heating rate							
	5 °C/min		10 °C/min		15 °C/min		20 °C/min	
	E (kJ/mol)	R	E (kJ/mol)	R	E (kJ/mol)	R	E (kJ/mol)	R
A_2	32.93	0.995	39.60	0.998	53.52	0.994	52.44	0.996
A_3	18.87	0.993	23.26	0.998	32.48	0.992	31.74	0.995
A_4	11.84	0.991	15.09	0.998	21.96	0.991	21.38	0.994
R_1	69.78	0.997	82.40	0.998	108.58	0.993	106.66	0.996
R_2	72.39	0.996	85.47	0.998	112.57	0.994	110.57	0.996
R_3	73.27	0.996	86.46	0.999	113.90	0.994	111.82	0.996
D_1	148.73	0.997	174.17	0.998	226.80	0.994	222.98	0.996
D_2	152.14	0.997	178.25	0.998	232.04	0.994	228.13	0.996
D_3	155.72	0.996	182.41	0.999	237.44	0.995	233.45	0.997
D_4	153.40	0.997	179.66	0.999	233.78	0.994	229.88	0.996
F_1	75.06	0.996	88.54	0.999	116.64	0.995	144.56	0.997
F_2	1.58	0.370	3.28	0.809	6.85	0.954	6.44	0.916
F_3	12.39	0.895	15.98	0.960	23.29	0.983	22.56	0.970

T a b l e 5

Activation energies obtained for several solid-state processes at different heating rates using the Tang method

Mechanism	Heating Rate							
	5 °C/min		10 °C/min		15 °C/min		20 °C/min	
	E (kJ/mol)	R	E (kJ/mol)	R	E (kJ/mol)	R	E (kJ/mol)	R
A_2	33.36	0.995	40.04	0.999	53.95	0.994	52.88	0.996
A_3	19.33	0.994	23.72	0.998	32.94	0.993	32.20	0.995
A_4	12.32	0.992	15.56	0.998	22.44	0.991	21.86	0.994
R_1	70.16	0.997	82.79	0.998	108.92	0.993	107.01	0.996
R_2	72.77	0.996	85.84	0.998	112.90	0.994	110.91	0.996
R_3	73.66	0.996	86.83	0.999	114.23	0.994	112.24	0.996
D_1	149.02	0.997	174.42	0.998	226.97	0.994	223.23	0.996
D_2	152.42	0.997	178.49	0.998	232.20	0.994	228.30	0.996
D_3	155.99	0.996	182.64	0.999	237.60	0.995	233.61	0.991
D_4	153.66	0.997	179.90	0.999	234.03	0.994	230.13	0.996
F_1	75.44	0.996	88.91	0.999	116.97	0.995	114.89	0.997
F_2	2.07	0.499	3.76	0.848	7.34	0.96	6.94	0.926
F_3	12.86	0.902	16.45	0.962	23.76	0.983	23.04	0.971

In particular, between D_n diffusion-type deceleration mechanisms, the activation energies corresponding to the D_1 one-dimensional diffusion-type deceleration mechanism is remarkable at a heating rate of 5 °C/min, as the closeness to the Kissinger and Flynn-Wall-Ozawa methods can be seen. When it is considered for the Coats-Redfern method, as given in Table 4, at a heating rate of 5 °C/min, the activation energy corresponding to the D_1 mechanism is 148.73 kJ/mol with a strong linear regression (R = 0.997). This value is very close to the value of 136.12 kJ/mol by the Flynn-Wall-Ozawa method and is also in good agreement with the Kissinger method (134.83 kJ/mol). Therefore, it can be said that the one-dimensional diffusion mechanism of D_1 is the probable thermodegradation kinetic mechanism of the poly(ICEMA) homopolymer according to the Coats-Redfern method.

T a b l e 6

Activation energies obtained for several solid-state processes at different heating rates using the Madhusudanan method

Mechanism	Heating rate							
	5 °C/min		10 °C/min		15 °C/min		20 °C/min	
	E (kJ/mol)	R	*E* (kJ/mol)	R	*E* (kJ/mol)	R	*E* (kJ/mol)	R
A_2	33.23	0.995	39.93	0.999	53.85	0.994	52.77	0996
A_3	19.22	0.993	23.61	0.998	32.83	0.993	32.09	0.995
A_4	12.20	0.991	15.44	0.998	22.31	0.991	21.74	0.994
R_1	70.08	0.997	82.71	0.998	108.89	0.993	106.98	0.996
R_2	72.68	0.996	85.71	0.998	112.79	0.994	110.80	0.996
R_3	73.57	0.996	86.79	0.999	114.20	0.994	112.13	0.996
D_1	149.01	0.997	174.42	0.998	227.00	0.994	223.18	0.996
D_2	152.41	0.997	178.49	0.998	232.23	0.994	228.33	0.996
D_3	155.98	0.996	182.65	0.999	237.63	0.995	233.64	0.997
D_4	153.58	0.997	179.82	0.999	233.98	0.994	230.07	0.996
F_1	75.36	0.996	88.87	0.999	116.86	0.995	114.79	0.997
F_2	1.95	0.469	3.64	0.839	7.21	0.958	6.82	0.924
F_3	12.75	0.900	16.33	0.961	23.65	0.983	22.92	0.971

T a b l e 7

Activation energies obtained for several solid-state processes at different heating rates using the Van Krevelen method

Mechanism	Heating rate							
	5 °C/min		10 °C/min		15 °C/min		20 °C/min	
	E (kJ/mol)	R	*E* (kJ/mol)	R	*E* (kJ/mol)	R	*E* (kJ/mol)	R
A_2	37.53	0.998	44.01	0.999	57.77	0.995	57.02	0.997
A_3	23.48	0.997	27.79	0.999	36.94	0.995	36.42	0.997
A_4	16.46	0.997	19.675	0.999	26.51	0.995	26.11	0.997
R_1	73.35	0.998	86,54	0.998	112.36	0.993	111.05	0.996
R_2	76.97	0.997	89,58	0.998	116.26	0.994	114.907	0.996
R_3	77.85	0.997	90,61	0.998	117.60	0.994	116.207	0.996
D_1	153.35	0.993	177.80	0.998	229.49	0.993	226.92	0.996
D_2	156.80	0.997	181.82	0.998	234.67	0.994	232.03	0.996
D_3	160.35	0.997	185.94	0.998	240.00	0.994	237.27	0.996
D_4	158.02	0.997	183.18	0.998	236.43	0.994	233.76	0.996
F_1	79.64	0.997	92.71	0.999	120.31	0.995	118.90	0.997
F_2	6.21	0.964	7.95	0.985	11.55	0.992	11.25	0.986
F_3	17.04	0.964	20.58	0.985	27.86	0.992	26.84	0.986

We have used the other integral methods of Tang, Madhusudanan and Van Krevelen to verify the D_1 mechanism determined by the Coats-Redfern method and also to increase the accuracy of the measurements. The calculated decomposition activation energies and linear regression values are listed in Tables 5, 6 and 7 for each method, respectively. Table 5 (Tang method) shows activation energy (E = 149.02 kJ/mol) and linear regression (R = 0.997) values corresponding to the D_1 mechanism at a heating rate of 5 °C/min, which are also in good agreement with the Flynn-Wall-Ozawa (E = 136.12 kJ/mol) and Kissinger (E = 134.83 kJ/mol) methods. Additionally, Table 6 gives similar results obtained by using the Madhusudanan method in which the activation energies and linear regressions for the D_1 mechanism at a heating rate of 5 °C/min are E = 149.01 kJ/mol and R = 0.997, respectively. Finally, the Van Krevelen method was tested. According to this method, the calculated activation energy (E = 153.35 kJ/mol) and regression (R = 0.997) at 5 °C/min are in good agreement with the Flynn-Wall-Ozawa and Kissinger methods, as shown by Table 7.

4. CONCLUSIONS

The thermal behaviors of poly(2-(isocoumarin-3-yl)-2-oxoethyl methacrylate) (poly(ICEMA)) were investigated by DSC and TGA techniques. The glass transition temperature of poly(ICEMA) was measured to be 161.69 ºC by DSC. The initial decomposition temperatures were increased from 256.59 to 286.10 °C as the heating rate increased to 20 ºC/min. The thermal decomposition activation energies of poly(ICEMA) in the conversion range of 7–19 % were found to be 136.12 and 134.83 kJ/mol by the Flynn–Wall–Ozawa and Kissinger methods, respectively. From the kinetic analysis of poly(ICEMA), the best conformity in all the kinetic models and the heating rates to that of the Flynn-Wall-Ozawa (E = 136.12 kJ/mol) and Kissinger (E = 134.83 kJ/mol) methods was obtained in the case of the Coats-Redfern method (E = 148.73 kJ/mol and R = 0.997) for the D_1 mechanism at a heating rate of 5 ºC/min. This result showed that the thermal decomposition mechanism of poly(ICEMA) proceeded at the optimum heating rate of 5 ºC/min over the D_1 one-dimensional diffusion-type deceleration mechanism.

Acknowledgements. We wish to thank the Adıyaman University Scientific Research Projects Unit (ADYÜBAP/FFYL2016-0003) for financially supporting this study.

REFERENCES

[1] S. Pal, V. Chatare, M. Pal, Isocoumarin and its derivatives: an overview on their synthesis and applications, *Curr. Org. Chem.* **15,** 782–800 (2011). DOI: 10.2174/138527211794518970.

[2] R. D. Barry, Isocoumarins. Development since 1950, *Chem. Rev.* **64,** 229–260 (1964). DOI: 10.1021/cr60229a002.

[3] E. Napolitano, Synthesis of isocoumarins over the last decade: a review, *Org. Prepn. Procedures Intl.* **29,** 631–664 (1997). DOI: 10.1080/00304949709355245.

[4] S. Pathak, D. Das, A. Kundu, S. Maity, N. Guchhait, A. Pramanik, Synthesis of 4-hydroxyindole fused isocoumarin derivatives and their fluorescence "Turn-off" sensing of Cu(II) and Fe(III) ions, *RSC Adv.* **5,** 17308–17318 (2015). DOI: 10.1039/c5ra01060h.

[5] P. Saikia, S. Gogoi, Isocoumarins: General aspects and recent advances in their synthesis, *Adv. Synth. Catal.* **360,** 2063–2075 (2018). DOI: 10.1002/adsc.201800019.

[6] K. Nozawa, M. Yamada, Y. Tsuda, K. Kawai, S. Nakajima, Synthesis of antifungal isocoumarins. II. Synthesis and antifungal activity of 3-substituted isocoumarins, *Chem. Pharm. Bull.* **29,** 2491–2495 (1981). DOI: https://doi.org/10.1248/cpb.29.2491.

[7] T. Furuta, Y. Fukuyama, Y. Asakawa, Polygonolide an İsocoumarin from polygonum-hydropiper possessing anti-inflammatory activity, *Phytochemistry*, **25,** 517–520 1986). DOI: https://doi.org/10.1016/S0031-9422(00)85513-2.

[8] H. Matsuda, H. Shimoda, M. Yoshikawa, Structure-requirements of isocoumarins, phthalides, and stilbenes from hydrangeae dulcis folium for inhibitory activity on histamine release from rat peritoneal mast cells, *Bioorg. Med. Chem.* **7,** 1445–1450 (1999). DOI: 10.1016/S0968-0896(99)00058-9.

[9] H. Sato, K. Konoma, S. Sakamura, Three new phytotoxins produced by Pyrenochaeta terrestris: pyrenochaetic acids A, B and C, *Agric. Biol. Chem.* **45,** 1675–1679 (1981). DOI: https://doi.org/10.1080/00021369.1981.10864745.

[10] A. C. Whyte, J. B. Glober, J. A. Scott, D. Mallock, Cercophorins A-C: Novel antifungal and cytotoxic metabolites from the coprophilous fungus cercophora areolata, *J. Nat. Prod.* **59,** 765–769 (1996). DOI: 10.1021/np9603232.

[11] Z. Essaidi, O. Krupka, K. Iliopoulos, E. Champigny, B. Sahraoui, M. Sallé, D. Gindre, Synthesis and functionalization of coumarin-containing copolymers for second order optical nonlinearities, O*pt. Mater.* **35,** 576–581 (2013). DOI: 10.1016/j.optmat.2012.10.011.

[12] T. Han, H. Q. Deng, C. Y. Y. Yu, C. Gui, Z. G. Song, R. T. K. Kwok, J. W. Y. Lam, B. Tang, Functional isocoumarin-containing polymers synthesized by rhodium-catalyzed oxidative polycoupling of aryl diacid and internal diyne, *Polym. Chem.* **7,** 2501–2510 (2016). DOI: 10.1039/c6py00206d.

[13] A. Kurt, M. Koca, Synthesis, characterization and thermal degradation kinetics of poly(3-acetylcoumarin-7-yl-

methacrylate) and its organoclay nanocomposites, *Journal of Engg. Research*, vol. **4**, no. 4**,** pp. 46–65 (2016).

[14] A. Kurt, O. K. Topsoy, Preparation of novel coumarin cyclic polymer/montmorillonite based nanocomposites, *Russ. J. Appl. Chem.* **90,** 2019−2027 (2017). DOI: 10.1134/S1070427217120199.

[15] A. Kurt, P. Yılmaz, Thermal decomposition kinetics of benzofuran derived polymer/organosilicate nanocomposites, *Kuwait J. Sci.* **43,** 172–184 (2016).

[16] Z. Barutçu, C. Kırılmış, A. Kurt, Synthesis, characterization and thermal decomposition kinetics of a novel benzofuran ketoxime derived polymer, *Acta Chim. Slov.* **62,** 428–436 (2015). DOI: 10.17344/acsi.2014.900.

[17] H. J. Patel, M. G. Patel, A. K. Patel, K. H. Patel, R. M. Patel, Synthesis, characterization and antimicrobial activity of important heterocyclic acrylic copolymers, *Express Polym. Lett.* **2,** 727–734 (2008). DOI: 10.3144/expresspolymlett.2008.86.

[18] M. Koca, A. S. Erturk, A. Umaz, Microwave-assisted intermolecular aldol condensation: Efficient one-step synthesis of 3-acetyl isocoumarin and optimization of different reaction conditions, *Arab. J. Chem.* **11,** 538–545 (2018). DOI: https://doi.org/10.1016/j.arabjc.2015.11.013.

[19] S. Fomine, E. Rivera, L. Fomina, A. Ortiz, T. Ogawa, Polymers from coumarines: 4. Design and synthesis of novel hyperbranched and comb-like coumarin-containing polymers, *Polymer*, **39,** 3551–3558 (1998), DOI: 10.1016/S0032-3861(97)10003-9

[20] X. L. Meng, Y. D. Huang, H. Yu, Z. S. Lv, Thermal degradation kinetics of polyimide containing 2,6-benzobisoxazole units, *Polym. Degrad. Stab.* **92,** 962–967 (2007). DOI: 10.1016/j.polymdegradstab.2007.03.005

[21] S. Vyazovkin, Thermal analysis, *Anal. Chem.* **78,** 3875–3886 (2006). DOI: 10.1021/ac0605546.

[22] S. Ma, J. O. Hill, S. Heng, A kinetic-analysis of the pyrolysis of some Australian coals by nonisothermal thermogravimetry, *J. Therm. Anal.* **37,** 1161–1177 (1991). DOI: 10.1007/BF01913852.

[23] Z. D. Zivkovic, J. Sestak, Kinetics and mechanism of the oxidation of molybdenum sulphide, *J. Therm. Anal. Calorim.* **53,** 263–267 (1998). DOI: 10.1023/A:1010108813595.

[24] J. H. Flynn, L. A. Wall, A quick, direct method for the determination of activation energy from thermogravimetric data, *J. Polym. Sci. B*, **4,** 323–328 (1966). DOI: https://doi.org/10.1002/pol.1966.110040504

[25] T. Ozawa, Applicability of Friedman plot, *J. Therm. Anal.* **31,** 547–551 (1986). DOI: 10.1007/BF01914230.

[26] H. E. Kissinger, Reaction kinetics in differential thermal analysis, *Anal. Chem.* **29,** 1702–1706 (1957). DOI: 10.1021/ac60131a045.

[27] A. W. Coats, J.P Redfern, Kinetic parameters from thermogravimetric data, *Nature*, **201,** 68–69 (1964). DOI:10.1038/201068a0

[28] W. Tang, Y. Liu, H. Zhang, C. Wang, New approximate formula for Arrhenius temperature integral, *Thermochim. Acta*, **408,** 39–43 (2003). DOI: 10.1016/S0040-6031(03)00310-1.

[29] P. M. Madhusudanan, K. Krishnan, K. N. Ninan, New equations for kinetic-analysis of nonisothermal reactions, *Thermochim. Acta*, **221,** 13–21 (1993). DOI: 10.1016/0040-6031(93)80519-G

[30] D. W. Van Krevelen, C. Van Herrden, F. J. Hutjens, Kinetic study by thermogravimetry, *Fuel*, **30,** 253–258 (1951).